SCIENTIFIC REPORTS

OPEN

SUBJECT AREAS:
ACOUSTICS
SURFACES, INTERFACES AND THIN FILMS

Received
12 August 2014

Accepted
2 October 2014

Published
23 October 2014

Correspondence and requests for materials should be addressed to H.C. (hchen@iphy.ac.cn)

Indium segregation measured in InGaN quantum well layer

Zhen Deng[1], Yang Jiang[1], Wenxin Wang[1], Liwen Cheng[2], Wei Li[1], Wei Lu[2], Haiqiang Jia[1], Wuming Liu[1], Junming Zhou[1] & Hong Chen[1]

[1]Beijing National Laboratory for Condensed Matter Physics, Institute of Physics, Chinese Academy of Sciences, Beijing 100190, China, [2]National Laboratory for Infrared Physics, Shanghai Institute of Technical Physics, Chinese Academy of Sciences, Shanghai 200083, China.

The indium segregation in InGaN well layer is confirmed by a nondestructive combined method of experiment and numerical simulation, which is beyond the traditional method. The pre-deposited indium atoms before InGaN well layer growth are first carried out to prevent indium atoms exchange between the subsurface layer and the surface layer, which results from the indium segregation. The uniform spatial distribution of indium content is achieved in each InGaN well layer, as long as indium pre-deposition is sufficient. According to the consistency of the experiment and numerical simulation, the indium content increases from 16% along the growth direction and saturates at 19% in the upper interface, which cannot be determined precisely by the traditional method.

The segregation phenomenon exists generally in kinds of compound semiconductor systems[1–8]. Due to the coherency strain and different miscibility between different materials, the atoms segregate into the upper layer, which will lead to the component nonuniform distribution of binary or ternary alloy[5–9]. This phenomenon changes the energy levels, which further influences the optical and electrical performances of semiconductor devices. Therefore, many techniques are performed to investigate it, such as secondary ion mass spectroscopy (SIMS)[4], transmission electron microscope (TEM)[5,10], X-ray photo-emission spectroscopy (XPS)[11], reflection high-energy electron diffraction (RHEED)[12], photoluminescence (PL)[13–16] and so on. Consequently, several segregation models are performed to analyze the atom content distribution[17–21].

In recent years, light emitting diodes (LEDs) and laser diodes (LDs) with InGaN/GaN multi quantum wells (MQWs) active region have been developed rapidly and used widely in varies of applications[22–28]. In the LED or LD structure, the optoelectronic properties are very sensitive to the indium content distribution in the InGaN well layer, and the physical mechanism is still in controversy. In the meantime, the indium segregation phenomenon in InGaN well layer has been studied for several years[29–34]. Due to the indium segregation, the nonuniform distribution of indium content will seriously change the potential profile of InGaN/GaN MQWs. These results reduce the overlap between the electron and hole wave functions in the InGaN well layer and hence decrease the internal quantum efficiency[29]. Therefore, it is necessary to realize the indium segregation extent exactly. However, as the researchers want to precisely measure the indium content profile in the InGaN well layer, the study on indium segregation runs into difficulties due to the slight change of indium content and lack of effective measurement method.

In this work, a novel design is performed to determine the indium segregation quantitatively in the InGaN well layer. This method can be nondestructive to ascertain the indium distribution profile in InGaN well layer. We first obtain the uniform spatial distribution of indium content by using indium pre-deposition (IP) before InGaN well layer growth. And then the indium content value at the upper interface of InGaN well layer is ascertained by the numerical simulation. After that, the indium content distribution in InGaN well layer is observed by electroluminescence (EL) experimental and theoretical simulation results.

Results

In our design, the InGaN well thickness of conventional LED A is 2.5 nm and the growth time is 2 min. LEDs B-D are grown under the same conditions. Nevertheless, IP before each InGaN well layer growth is introduced and the time of pre-deposition is 1.5, 2, 2.5 min respectively. A growth interruption time of 30 seconds is also performed after the growth of GaN barrier layer. The structure diagram of all the LEDs is shown in Fig. 1(a). Figure 1(b) shows (0002) plane diffraction obtained with $\omega/2\theta$ scans along the growth direction for the MQWs. More details

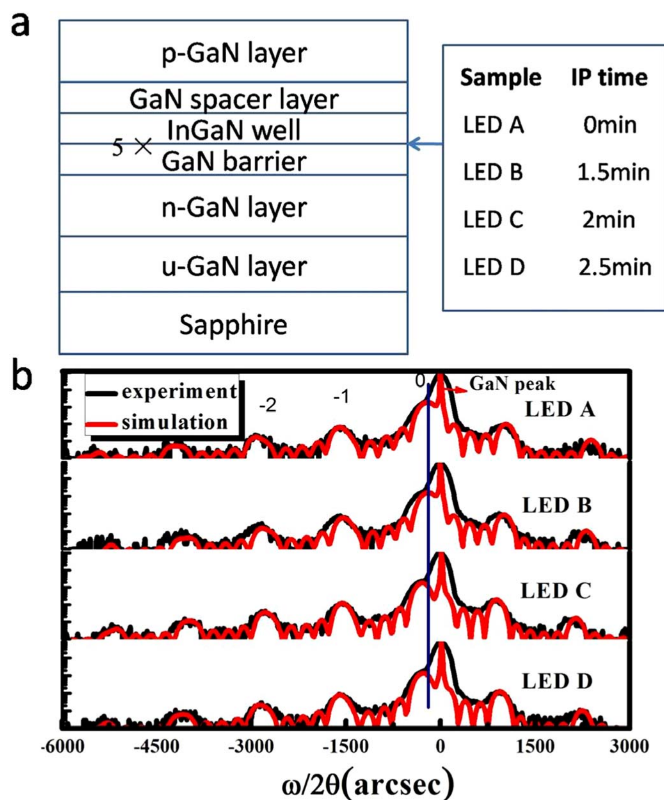

Figure 1 | (a) The structure diagram of all the LEDs and (b) (0002) plane ω/2θ HRXRD spectra of InGaN/GaN MQWs with different IP time.

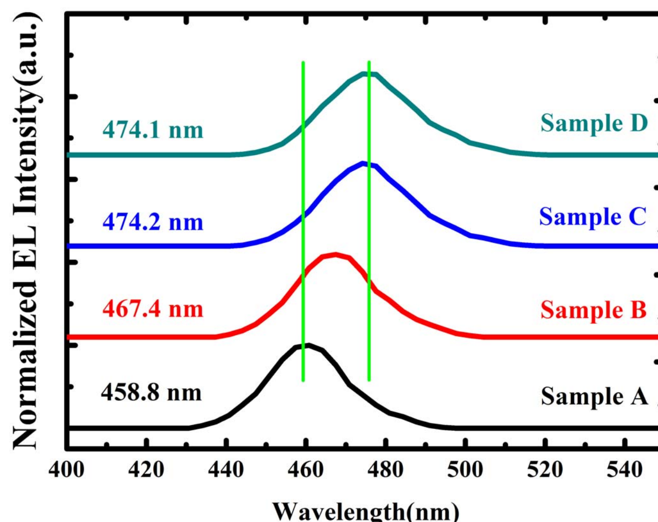

Figure 2 | Room-temperature EL spectra (1 mA) for LEDs A–D. The major emission peak wavelengths for LEDs A–D are 458.8, 467.4, 474.2, 474.1 nm, respectively.The two green lines show a redshift of ~15.4 nm, as the IP time increases.

of high resolution X-ray diffraction (HRXRD) data analysis can be found in Ref. 35. Compared to LED A, the Indium content increases slightly in the InGaN well layer for LEDs B–D due to IP effect, while the thicknesses of GaN barrier and InGaN well layers for all the LEDs are almost the same. Moreover, The FWHM values of the InGaN "+1st" diffraction peak for the LEDs A–D are 267, 223, 201, 204 arcsec, respectively, and the values for LEDs B–D are much smaller than that of LED A, which suggests that the uniformity of indium content distribution is improved due to the indium pre-deposition. Besides, It is also noted that the high series satellite peaks of LEDs B–D is more distinct than that of LED A, which shows that the structure properties are significantly improved with IP process. These results indicate that no InN or island is formed. It is because the indium pre-deposition is performed at a temperature of 730°C, higher than the InN growth temperature which is usually under 550°C.

The EL spectra are measured for all the LEDs under 1 mA injection current. Figure 2 reveals that the major emission peak wavelengths for LEDs A–D are 458.8, 467.4, 474.2, 474.1 nm, respectively. According to the variation of peak wavelength, it is observed that the peak wavelength red-shift (~15.4 nm) with the increase of the IP time for the LEDs A–D. This EL red-shift is consistent with our former HRXRD analysis of IP effect. During the IP process, most of the deposited indium is taken away by the gas flow in the reactor, while part of indium remains on the wafer and generates an "indium floating layer"[19,20]. The "indium floating layer" could prevent atoms exchange between the surface layer and subsurface layer, which reduces the effect of indium segregation. As longer pre-deposition time is performed, more indium atoms adsorb on the surface of GaN layer and these atoms are always exchange into the upper layer due to the lower energy of the surface in the following InGaN growth. As a result, more indium atoms incorporate into the InGaN films leading to the red-shift of emission peaks in EL measurement. We also note that though the IP time of LED C and D are 2 min and 2.5 min, respectively, their EL peak wavelengths are nearly the same. The unchanged wavelength with increasing IP time provides evidence for the saturation of indium content in the InGaN well layers. By 2-min IP time, the number of indium atoms is enough to totally occupy the low-energy states on the GaN surface layer. Consequently, the indium atoms exchange between the subsurface and surface layers keeps dynamic balance and the segregation is completely suppressed in the following InGaN layer growth. As a result, the spatial distribution of indium content is uniform in the each InGaN well layer, as long as IP is sufficient. It is another difference with InGaAs system, the excess indium pre-deposition will lead to a higher indium content distribution at the lower part of InGaAs layers.

Now we have shown that the indium content reaches saturation in the condition of 2 min IP time. The further question is how does indium content distribute along growth direction in InGaN well due to the segregation for LED A.

It has been demonstrated that the indium content varies exponentially along the growth direction in InGaAs materials. According to exponential model, the indium content in the ***n***th monolayer in the InGaAs materials is given in the form;

$$x_n = x_0(1\text{-}R^n)(1 \leq n \leq N;\ \text{well}) \tag{1}$$

$$R = \exp(\text{-}d/\lambda) \tag{2}$$

In our case, we hereby build the model about the indium segregation of the conventional LED structure in the following form:

$$y = a * (1\text{-}e^{\text{-}cx}) \tag{3}$$

where y is the indium content, x is the distance from the lower interface, and a is a constant. In addition, c is a coefficient about the indium segregation length. Because the indium content of the upper interface of InGaN well makes not much difference to the lower interface and the thickness of InGaN well is very small, the above equation can be simplified as follows:

$$y \approx y_1 * x + y_0 \tag{4}$$

where y_0 is the indium content at lower interface of InGaN well layer and y_1 is the slope. So the exponential model has been replaced by the linear one. The schematic indium content profiles of the MQWs for

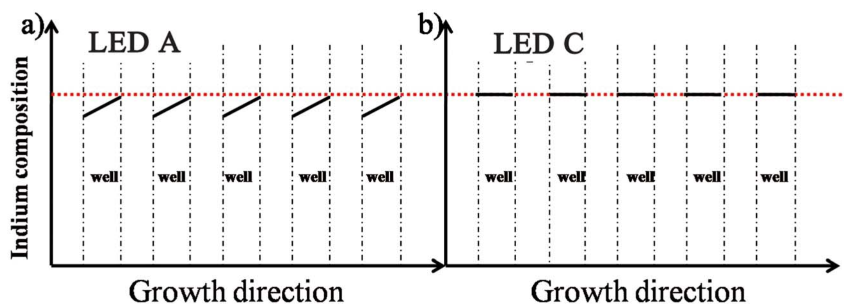

Figure 3 | The indium content distribution charts of the MQWs in the active region for LED A and LED C. a): the indium content increases along the growth direction for LED A; b) the indium content is consistent for LED C. In the meanwhile, the indium composition at the upper layer of sample A is the same with indium content of InGaN well layer of LED C.

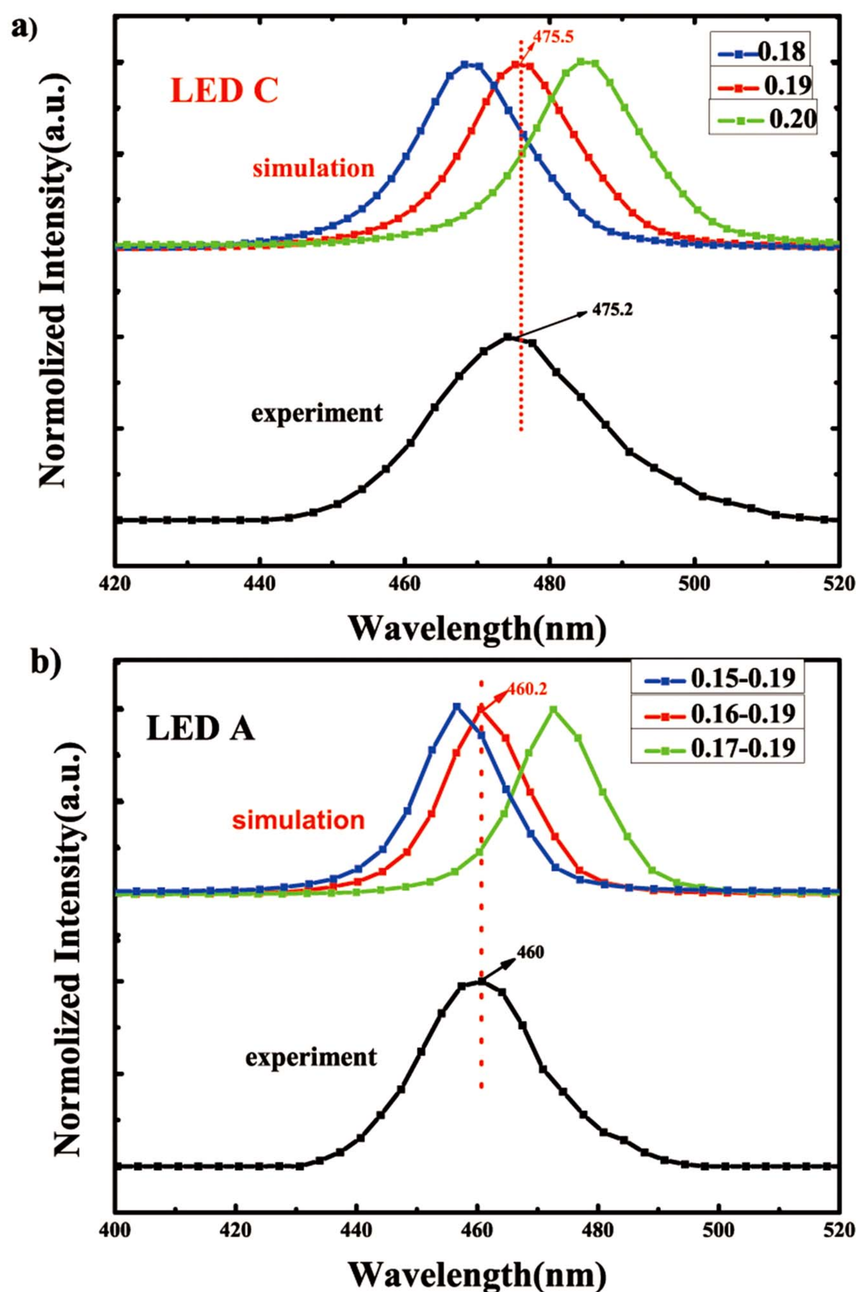

Figure 4 | The calculated and experimental EL spectra (1 mA) of the LED A and LED C. The calculated EL spectra with different indium distribution are shown as color line and the experimental EL spectra is shown as black line. Based on the data consistency of the experiment and numerical simulation, the indium content is ~19%, while the indium content increases from ~16% along the growth direction and saturates at ~19% in the upper interface of InGaN well layer.

LED A and LED C are shown in Fig. 3(a) and Fig. 3(b), respectively. The indium content in the conventional structure increases along with the growth direction of InGaN well layer due to the indium segregation, while the indium content is constant in the structure with IP process.

During the InGaN growth in MOCVD system, the indium incorporation efficiency is poor and most of the indium atoms are desorbed at growth temperature (730°C). For example, in our experiment, the ratio of Ga/In is usually about 1 : 1, but the indium content in the InGaN well layer is much smaller than 0.5. The excess indium has the similar effect of IP, filling the low-energy states on the surface. In our design, the growth time of indium well layer is also 2 min. As mentioned above, 2-min IP time provides enough indium to balance the atom exchange, which means that there should be enough indium atoms to make the upper interface of InGaN well layer saturated, even without IP (LED A). As indicated by the red dotted line in Fig. 3, we can conclude that the indium content difference of the upper interface of InGaN well layer for LED A and LED C is slight, since the indium contents of upper surfaces in both samples are saturated.

LED devices with conventional structure (LED A) and IP structure (LED C) are fabricated and characterized by EL spectra measurement. Besides, theoretical simulations of two LED structures are also carried out by Crosslight software. For LED C, the indium is uniformly distributed, so the square quantum well structure is adopted in the simulation where the indium content is the only unknown. The indium content can be obtained by fitting the simulated EL spectral to the experimental one, which is 19% (Fig. 4(a)). Based on above analysis, the indium content at upper interface of InGaN/GaN MQWs is also 19% for LED A. Another simulation for LED A is carried out. Triangle-shaped quantum well structure is used because the indium content is assumed to increase with InGaN layer thickness. Since the indium content at upper interface is known as 19%, the indium content at lower interface can be fitted similarly by comparing the simulated and experimental results, as shown in Fig. 4(b). When the indium content at the lower interface in InGaN well layer is 16%, the calculated spectrum agrees with that of the experiment. As a result, the influence of indium segregation on the content distribution can be obtained. For the conventional InGaN blue LED structures in our experiment, the indium content increases from 16% to 19% along the growth direction because of the indium segregation effect.

Discussion

In the light of the above, we have obtained the indium content profile in the InGaN well layer. It is noteworthy to mention here that due to the typical InGaN well thickness (~2.5 nm) and the slight indium content change in the InGaN well layer, the indium segregation cannot be accurately measured by the conventional method, such as TEM, SIMS, and so on[36–38]. Due to indium segregation, the non-uniform components distribution will lead to the local polarization effect and then influence the properties of optoelectronic devices. The new method is nondestructive to present a better understanding of indium segregation, which should be taken into consideration in the epitaxial growth process.

In conclusion, we have first developed a new method to determine the indium segregation in InGaN well layer. The effect of IP prior to the InGaN well growth on the indium content profile is demonstrated. As IP is sufficient, the uniform spatial indium content profile is realized in each InGaN well layer. Based on EL experiment and theoretical simulation results, the indium content increases from 16% along the growth direction and saturates at 19% in the upper interface of InGaN well layer. This method established in our work can describe the segregation behavior, which will enhance the better understanding of state densities, energy band and polarization effect in optoelectronic devices or microelectronic devices.

Methods

All growths are performed on 2-in (0001) sapphire substrates by low-pressure metal organic chemical vapor deposition (MOCVD). The precursors are trimethylgallium (TMGa), triethylgallium (TEGa), trimethylindium (TMIn), and ammonia (NH_3), respectively. Prior to the growth of GaN nucleation layers (NLs), the substrates are exposed to hydrogen (H_2) at 1100°C to desorb surface contaminants for 12 min. The temperature is lowered to 550°C and 25 nm thick GaN NLs are deposited using TMGa and NH_3. These NLs are subsequently annealed in NH_3 and H_2, following the growth of 2.5 μm thick planar GaN layers at 1100°C. Then 3 μm-thick Si doped n type GaN layers are deposited at 1100°C, followed by the five periods of InGaN/GaN MQWs. The growth temperature of GaN barrier and InGaN well layer are 830°C and 730°C, respectively. Finally the 200 nm thick Mg-doped p-type GaN layer is deposited and the samples are annealed for 20 min to activate Mg ion in the nitrogen atmosphere at 700°C. In the whole deposition process, H_2 is used as an ambient gas for GaN layer, while N_2 is used as an ambient gas for the growth of InGaN/GaN MQWs to increase the indium incorporation efficiency. The rate of the indium flow is 93 μmol/min. Compared to LED A, LEDs B–D are distinguished by adopting IP time. For LEDs B–D, prior to the growth of each InGaN QW layer, indium atoms are deposited and the deposition time is 1.5, 2, and 2.5 min, respectively. A growth interruption time of 30 seconds is also performed after the growth of GaN barrier layer.

Then the epitaxial chips are fabricated from these structure using standard mesa etching and contact fabrication techniques. The fabrication of the LED chips with a device area of 300*300 μm^2 is described in detail elsewhere. The LED chips are then mounted on a Cu cold stage. Then the EL spectra of all samples under 1 mA current injection levels are obtained in pulsed mode with a duty cycle of 10% and a pulse length of 20 ms. At the same time, the simulation is carried out to calculate the EL spectra according to the new model by the Crosslight software.

1. Copel, M., Reuter, C., Kaxiras, E. & Tromp, R. M. Surfactants in epitaxial growth. *Phys. Rev. Lett.* **63**, 632–635 (1989).
2. Iyer, S. S., Tsang, J. C., Copel, M. W., Pukite, P. R. & Tromp, R. M. Growth temperature dependence of interfacial abruptness in Si/Ge heteroepitaxy studied by Raman spectroscopy and medium energy ion scattering. *Appl. Phys. Lett.* **54**, 219–221 (1989).
3. Fukatsu, S., Fujita, K., Yaguchi, H., Shiraki, Y. & lto, R. Self-limitation in the surface segregation of Ge atoms during Si molecular beam epitaxial growth. *Appl. Phys. Lett.* **59**, 2103–2105 (1991).
4. Muraki, K., Fukatsu, S., Shiraki, Y. & Ito, R. Surface segregation of In atoms during molecular beam epitaxy and its influence on the energy levels in InGaAs/GaAs quantum wells. *Appl. Phys. Lett.* **61**, 557–559 (1992).
5. Bormann, I. *et al.* Midinfrared intersubband electroluminescence of Si/SiGe quantum cascade structures. *Appl. Phys. Lett.* **80**, 2260–2262 (2002).
6. Moon, Y. T. *et al.* Effects of thermal and hydrogen treatment on indium segregation in InGaN/GaN multiple quantum wells. *J. Appl. Phys.* **89**, 6514–6518 (2001).
7. Grandjean, N. *et al.* GaInN/GaN multiple-quantum-well light-emitting diodes grown by molecular beam epitaxy. *Appl. Phys. Lett.* **74**, 3616–3618 (1999).
8. Ludwig, C. D. R., Gruhn, T. & Felser, C. Indium-Gallium Segregation in $CuIn_xGa_{1-x}Se_2$: An Ab Initio-Based Monte Carlo Study. *Phys. Rev. Lett.* **105**, 025702 (2010).
9. Duxbury, N. *et al.* Indium segregation in InGaN quantum-well structures. *Appl. Phys. Lett.* **76**, 1600–1602 (2000).
10. Ramaiah, K. S. *et al.* Studies of InGaN/GaN multiquantum-well green-light-emitting diodes grown by metalorganic chemical vapor deposition. *Appl. Phys. Lett.* **85**, 401–403 (2004).
11. Moison, J. M. *et al.* Surface segregation in III–V alloys. *J. Cryst. Growth.* **111**, 141–150 (1991).
12. Gerard, J. M. & Anterroches, C. D. Growth of InGaAs/GaAs heterostructures with abrupt interfaces on the monolayer scale. *J. Cryst. Growth.* **150**, 467–472 (1995).
13. Martin, J. Y. & Gerard, J. M. Monolayer-scale optical investigation of segregation effects in semiconductor heterostructures. *Phys. Rev. B.* **45**, 6313 (1992).
14. Sato, M. & Horikoshi, Y. Effect of indium replacement by gallium on InAs/GaAs quantized levels. *Surf. Sci.* **267**, 195–198 (1992).
15. Muraki, K., Fukatsu, S., Shiraki, Y. & Ito, R. Surface segregation of In atoms and its influence on the quantized levels in InGaAs/GaAs quantum wells. *J. Cryst. Growth.* **127**, 546–549 (1993).
16. Schowalter, M., Rosenauer, A. & Gerthsen, D. Influence of surface segregation on the optical properties of semiconductor quantum wells. *Appl. Phys. Lett.* **88**, 111906 (2006).
17. Liao, X. Z., Zou, J., Cockayne, D. J. H., Leon, R. & Lobo, C. Indium Segregation and Enrichment in Coherent In_xGa_{1-x} As/GaAs Quantum Dots. *Phys. Rev. Lett.* **82**, 5148 (1999).
18. Kaspi, R. & Evans, K. R. Improved compositional abruptness at the InGaAs on GaAs interface by presaturation with In during molecular-beam epitaxy. *Appl. Phys. Lett.* **67**, 819–821 (1995).
19. Chattopadhyay, K. *et al.* Electroreflectance study of effects of indium segregation in molecular-beam-epitaxy-grown InGaAs/GaAs. *J. Appl. Phys.* **81**, 3601–3606 (1997).

20. Litvinov, D. *et al.* Transmission electron microscopy investigation of segregation and critical floating-layer content of indium for island formation in $In_xGa_{1-x}As$. *Phys. Rev. B* **74**, 165306 (2006).
21. Cho, J. H., Zhang, S. B. & Zunger, A. Indium-Indium Pair Correlation and Surface Segregation in InGaAs Alloys. *Phys. Rev. Lett.* **84**, 3654 (2000).
22. Nakamura, S. The Roles of Structural Imperfections in InGaN-Based Blue Light-Emitting Diodes and Laser Diodes. *Science* **281**, 956–961 (1998).
23. Tran, C. A. *et al.* Phase separation in InGaN/GaN multiple quantum wells and its relation to brightness of blue and green LEDs. *J. Crystal. Growth.* **195**, 397–400 (1998).
24. Ponce, F. A. & Bour, D. P. Nitride-based semiconductors for blue and green light-emitting devices. *Nature* **386**, 351–359 (1997).
25. Nagahama, S., Yanamoto, T., Sano, M. & Mukai, T. Characteristics of InGaN laser diodes in the pure blue region. *Appl. Phys. Lett.* **79**, 1948–1950 (2001).
26. Kojima, K. *et al.* Gain suppression phenomena observed in $In_xGa_{1-x}N$ quantum well laser diodes emitting at 470 nm. *Appl. Phys. Lett.* **89**, 241127 (2006).
27. Zhu, D., Wallis, D. J. & Humphreys, C. J. Prospects of III-nitride optoelectronics grown on Si. *Rep. Prog. Phys.* **76**, 106501 (2013).
28. Akasaki, I. & Amano, H. Breakthroughs in Improving Crystal Quality of GaN and Invention of the p–n Junction Blue-Light-Emitting Diode. *Jpn. J. Appl. Phys.* **45**, 9001–9010 (2013).
29. Mayrock, O., Wunsche, H. J. & Henneberger, F. Polarization charge screening and indium surface segregation in (In,Ga)N/GaN single and multiple quantum wells. *Phys. Rev. B.* **62**, 16870 (2000).
30. Jinschek, J. R., Erni, R., Gardner, N. F., Kim, A. Y. & Kisielowski, C. Local indium segregation and bang gap variations in high efficiency green light emitting InGaN/GaN diodes. *Solid State Commun.* **137**, 230–234 (2006).
31. Klymenko, M. V., Shulika, O. V. & Sukhoivanov, I. A. Theoretical study of optical transition matrix elements in InGaN/GaN SQW subject to indium surface segregation. *IEEE.* **17**, 1374–1380 (2011).
32. Lei, H. P., Chen, J. & Ruterana, P. Role of c-screw dislocations on indium segregation in InGaN and InAlN alloys. *Appl. Phys. Lett.* **96**, 161901 (2010).
33. Feng, Z. C. *et al.* Photoluminescence characteristics of low indium composition InGaN thin films grown on sapphire by metalorganic chemical vapor deposition. *Thin Solid Films.* **498**, 118–122 (2006).
34. Walther, T., Amari, H., Ross, I. M., Wang, T. & Cullis, A. G. Lattice resolved annular dark-field scanning transmission electron microscopy of (Ag,In)GaN/GaN layers for measuring segregation with sub-monolayer precision. *J Mater Sci.* **48**, 2883–2892 (2013).
35. Deng, Z. *et al.* A novel wavelength-adjusting method in InGaN-based light emitting diodes. *Sci. Rep.* **3**, 3389 (2013).
36. Pereira, S. *et al.* Strain and composition distributions in wurtzite InGaN/GaN layers extracted from x-ray reciprocal space mapping. *Appl. Phys. Lett.* **80**, 3913–3915 (2002).
37. Li, T. *et al.* Indium redistribution in an InGaN quantum well induced by electron-beam irradiation in a transmission electron microscope. *Appl. Phys. Lett.* **86**, 241911 (2005).
38. Martini, S. *et al.* Influence of indium segregation on the RHEED oscillations during the growth of InGaAs layers on a GaAs(0 0 1) surface. *J. Crystal. Growth.* **251**, 101–105 (2003).

Acknowledge

Supported by National High Technology Research and Development Program of China (grant nos. 2011AA03A112 and 2011AA03A106) and National Nature Science Foundation (grant nos. 11204360 and 61210014).

Author contributions

H.C. and Y.J. conceived and directed the research. Z.D. carried out all the wafers growth experiments, chips fabrication and characterization test. In the meanwhile, Z.D. and L.C. carried out the simulation by the Crosslight software. In the end, Z.D. wrote the main manuscript text and all the authors reviewed the manuscript.

Additional information

Competing financial interests: The authors declare no competing financial interests.

How to cite this article: Deng, Z. *et al.* Indium segregation measured in InGaN quantum well layer. *Sci. Rep.* **4**, 6734; DOI:10.1038/srep06734 (2014).

This work is licensed under a Creative Commons Attribution-NonCommercial-ShareAlike 4.0 International License. The images or other third party material in this article are included in the article's Creative Commons license, unless indicated otherwise in the credit line; if the material is not included under the Creative Commons license, users will need to obtain permission from the license holder in order to reproduce the material. To view a copy of this license, visit http://creativecommons.org/licenses/by-nc-sa/4.0/